ELSEVIER

Journal of Molecular Liquids 135 (2007) 75–85

journal of MOLECULAR LIQUIDS

www.elsevier.com/locate/molliq

Water phases under high electric field and pressure applied simultaneously

I. Danielewicz-Ferchmin [a], E. Banachowicz [a], A.R. Ferchmin [b,*]

[a] *Faculty of Physics, A. Mickiewicz University, Umultowska 85, PL-61-614 Poznań, Poland*
[b] *Institute of Molecular Physics, Polish Academy of Sciences, M. Smoluchowskiego 17, PL-60-179 Poznań, Poland*

Received 24 January 2006; accepted 25 October 2006
Available online 28 February 2007

Abstract

The rigorous equation of state of an open system containing water in an electric field above 10^8 V m^{-1} under pressure applied in the range $10^{-4} \le P_o \le 0.8$ GPa leads to phase diagrams with two possible kinds of phase transitions at 293 K. The first one is the discontinuous phase transition under pressure applied in the range $10^{-4} \le P_o \le 0.05$ GPa in the Π, σ coordinates (Π is the electrostriction pressure and σ denotes the surface charge density at an adjacent charged surface). The second one represents the continuous phase transition under pressure applied in the range $10^{-4} \le P_o \le 0.8$ GPa; it occurs at higher values of σ than the former one.

PACS: 05.70.Np; 68.35.Rh; 77.22.−d; 77.22.Ch
Keywords: Water; Electrochemistry; Phase diagram; Thermodynamics

1. Introduction

Water is known for its rich phase diagram in the *P*, *V*, *T* variables. However, our knowledge of H_2O phases under the action of high electric fields $E > 10^8$ V m^{-1} seems to remain still in its infancy and only a few isolated experimental facts are known [1–7] accompanied by a number of theoretical approaches to the question. Thus, any attempt to clarify the situation seems substantiated. The electric fields above 10^8 V m^{-1} can be encountered, e.g., in hydration layers arising when charged surfaces with surface (free) charge density $\sigma_o \ge 10^{-3}$ C m^{-2} are immersed in water. Such charge densities can exist at the surfaces of flat [4] or spherical (mercury droplets) [1,2] metallic electrodes, oxides, for instance TiO_2 [3] and RuO_2 [6], at surfaces of proteins [8–12] and micelles as well as at internal surfaces of reverse micelles [13]. High local electric fields exist also around ions in solutions.

In this paper the properties of water in a high electric field above 10^8 V m^{-1} in various conditions specified by temperature and pressure applied are discussed. Our earlier effort has been concentrated on establishing the effect of high electric field on the properties of water (at that time solely under atmospheric pressure), and in particular the coexistence of its different phases [14,15]. The most striking earlier result was the finding of a region of coexistence of two water phases (B and A) under various temperatures together with a corresponding "electric" critical point. A literature experiment apparently confirmed the existence of the latter [1,2]. Herein, we discuss what happens to the same system under the action of externally applied pressure of the order of tens or hundreds of MPa. It will be shown that at ambient temperature under various moderate pressures of several tens of MPa one also finds a region of coexistence of two phases (related to a first-order, discontinuous phase transition) and a corresponding critical point.

The discussion is based on the statistical and thermodynamic approach [15] taking into account the dipoles of water molecules. The current analysis leads to predictions of some new effects in water in the electric field under pressure. We find a discontinuous transition induced by electric field at various pressures. The knowledge of the permittivity ϵ is needed to evaluate the local electrostriction pressure Π [16] under the pressure P_o applied. The approach of Refs. [17,18] is applicable to ϵ of water in high electric fields and in the temperature and pressure range in which H_2O is liquid. The electrostriction pressure coefficient is introduced, defined by the slope γ of the Π vs. σ isotherms. Yet another possible second order (continuous) phase transition with the related order parameter $\langle \cos\theta \rangle$ (mean cosine between the electric field and

* Corresponding author. Tel.: +48 61 8695123; fax: +48 61 8684524.
E-mail address: arfer@ifmpan.poznan.pl (A.R. Ferchmin).

0167-7322/$ - see front matter © 2007 Published by Elsevier B.V.
doi:10.1016/j.molliq.2006.10.006

dipole moment of the H_2O molecule) is deduced from the behaviour of γ. The results confirm the reputation of water as a substance of a very complex phase behaviour.

2. Reasons for and consequences of the flow of the dipolar water molecules into the high electric field region

In this section, for the sake of completeness, some details of derivation of the equation of state (called thermodynamic or rigorous [19]) of H_2O in an open system already presented in Ref. [15], are given. The equation of state makes a basis for a discussion of the pressure and thermal behaviour of H_2O in high electric field.

2.1. Equilibrium condition

The chemical potential of a water molecule, placed in a high electric field at the cost of the work W needed for reorienting its dipole, is reduced by ζ_W with respect to that of a molecule outside the electric field. Actually, only those dipoles of H_2O molecules in the closest vicinity of the charged surface are exposed to the very high field as the electric field strength E falls down dramatically with increasing distance from this surface. Thus, no reorientation work W is done on the dipoles of H_2O molecules situated far enough from the charged surface. There is no wall impermeable to H_2O molecules between the part of water close to the charged surface, hence within the reach of the high field E, and that outside the reach of E. It follows that the part of water in the field E is an open subsystem. Since the chemical potential of a water molecule is reduced locally, a gradient of the chemical potential arises. The existence of this gradient implies the lack of equilibrium of the whole. As a consequence, a flow of dipolar molecules into the high electric field region arises. It is called the pull of dipoles into the field. The increase in the number of molecules in the field means a marked increase in the local mass density (electrostriction). On the other hand, the same increase in the mass density can be achieved by applying an external hydrostatic pressure. The pressure leading to an increase in the mass density equal to that due to electrostriction is called the electrostriction pressure. The pull of dipoles into the field ultimately leads to a new thermodynamic equilibrium state. We are interested in a new equilibrium state reached as a result of this process, say, in the double layer or in the hydration shells of ions. The work L related to water compression in the electric field, i.e., the electrostriction work, enhances the chemical potential of a water molecule by ζ_L. After reaching the equilibrium, the latter compensates the negative increment ζ_W

$$-\zeta_W = \zeta_L. \tag{1}$$

2.2. The rigorous equation of state of H_2O expressed in the Π, σ, T variables

The change in the chemical potential ζ_W is calculated in a way similar to that described earlier [20–22]. In the immediate neighbourhood of the charged surface the field strength E is

$$E = \frac{\sigma_o}{\epsilon_o} = \frac{\sigma}{\epsilon\epsilon_o}, \tag{2}$$

where σ_o is the surface (free) charge density, ϵ is the permittivity, ϵ_o is the permittivity of vacuum. Similarly, the strength E of the field around the ions (Coulomb field) is given by Eq. (2) where

$$\sigma = \frac{q}{4\pi x^2}, \tag{3}$$

q is the elementary charge, x is the reduced distance from the centre of the ion $x = r \times |Z|^{-1/2}$, r is the distance from the centre of the ion and Z is the number of excess elementary charges of an ion (valence). The work W done by the electric field is [20,22]

$$W = \frac{V}{\epsilon_o}\int_0^Y \frac{\sigma}{\epsilon}\mathrm{d}y, \text{ where } y = \sigma\left(1-\frac{1}{\epsilon}\right). \tag{4}$$

V is the volume of the subsystem in the field, $V\mathrm{d}y$ is the increment of the polarization of the volume V. The increment of the grand potential Ω is

$$\mathrm{d}\Omega = -S\mathrm{d}T + EV\mathrm{d}y - N\mathrm{d}\zeta_L, \tag{5}$$

where N is the number of molecules in the volume V. Let us introduce the notation

$$f = \int_0^Y \frac{\sigma}{\epsilon}\mathrm{d}y. \tag{6}$$

The work W performed leads to a change $\Delta\Omega$ in the value of the grand potential Ω of water

$$\left(\Delta\Omega\right)_{T,V,\zeta_L} = \frac{V}{\epsilon_o}f. \tag{7}$$

For ζ_W — the change in ζ as a result of the work W — one obtains

$$\zeta_W = \left(\frac{\partial\Omega}{\partial N}\right)_{T,V,\zeta_L}. \tag{8}$$

The increment

$$\zeta_W = \frac{v^o N^o}{\epsilon_o}\left(\frac{\partial f}{\partial N}\right)_{\zeta_L}, \tag{9}$$

where $v^o = V/N^o$ and N^o is the Avogadro number. As follows from Eq. (9)

$$\frac{\zeta_W}{v^o} = \frac{1}{\epsilon_o}\left[\left(\frac{\partial f}{\partial Y}\right)\left(\frac{\partial Y}{\partial \epsilon}\right)\right]_{\zeta_L} N^o\left(\frac{\partial \epsilon}{\partial N}\right)_Y. \tag{10}$$

The factors on the rhs of Eq. (10) are calculated in Appendix A. The derivatives in Eq. (10) are obtained on the basis of the statistical model approach to the permittivity of hydrogen

bonded liquids (including water) proposed earlier [17] valid in the range $273<T<373$ K. The mean cosine $\langle\cos\theta\rangle$ of the angle θ between the direction of the electric field E and the electric dipole moment μ of the water molecule for an arbitrary number I of allowed orientations of a dipole is expressed by the Brillouin function [23,24]

$$B_I(\Xi)=\frac{I}{I-1}\coth\frac{I\Xi}{I-1}-\frac{1}{I-1}\coth\frac{\Xi}{I-1}, \tag{11}$$

where Ξ is defined as

$$\Xi=\frac{AX}{T(\epsilon+n^2/2)}, \tag{12}$$

where $X=x^{-2}$ and

$$A=\frac{\mu q(n^2+2)}{8\pi k\epsilon_o}\ \mathrm{m^2\ K} \tag{13}$$

where k is the Boltzmann constant and n — refraction index. In the framework of our approach [17] the reorientations of the dipoles responsible for the high dielectric constant of water can be conceived as due to simultaneous shifts of the proton positions. The question if the structure of the neighbourhood of a hydrogen bonded molecule is described in the traditional way (with fourfold coordination), or according to a recent study — forming chains (with two-fold strongly bonded coordination [25]), plays a secondary role. In the range $273<T<373$ K, the hydrogen bond energy (20–25 kJ $\mathrm{mol^{-1}}$) exceeds the thermal energy (≈2–3 kJ $\mathrm{mol^{-1}}$) by a factor of about 10. Hence, the concept of two possible orientations ($I=2$) of water dipoles at ambient conditions seems to be justified. At very high temperatures, in which the thermal energy becomes comparable to the hydrogen bond energy ($T\approx3000$ K, $RT\approx25$ kJ $\mathrm{mol^{-1}}$) most of the hydrogen bonds should be broken and the dipoles should be able to rotate freely ($I=\infty$), which would induce a behaviour described by the Langevin function $L(\Xi)$. The form of $L(\Xi)$ is obtained from the Brillouin function $B_I(\Xi)$ in the limit ($I\to\infty$). In this context it is natural to look for an interpolation scheme between the two extremes of $\tanh(\Xi)$, corresponding to $I=2$, and $L(\Xi)$, corresponding to $I=\infty$, which represent the upper bound and the lower bound of $\langle\cos\theta\rangle$, respectively. One of the possible interpolation schemes goes as follows. It is conceivable that in the intermediate temperature range some hydrogen bonds are disrupted, which implies an intermediate number I of probable directions of the dipole moments lying between two extremes: $2<I<\infty$. Details of obtaining values of I at a given temperature can be found in Appendix B.

Let us now consider the change in the chemical potential ζ_L due to the compression work L which, according to Eq. (1), shall compensate ζ_W. The compression work L is calculated, similarly as in Refs. [20,26], by integrating the area under the isotherm $V=V(P)$ with P — pressure

$$L=\int_{P_o}^{P_i}V(P)\mathrm{d}P. \tag{14}$$

The change in the chemical potential ζ_L due to this work is

$$\zeta_L=\frac{\partial}{\partial N}\int_{P_o}^{P_i}V(P)\mathrm{d}P=\int_{P_o}^{P_i}v(P)\mathrm{d}P, \tag{15}$$

where P_o denotes the external pressure applied and P_i is the local pressure in the electric field. One can re-write Eq. (1) in the form

$$-\frac{\zeta_W}{v^o}=\frac{\zeta_L}{v^o}, \tag{16}$$

which, taking into account Eqs. (10) and (15), is the same as

$$-\frac{N^o}{\epsilon_o}\left[\left(\frac{\partial f}{\partial Y}\right)\left(\frac{\partial Y}{\partial\epsilon}\right)\right]_{\zeta_L}\left(\frac{\partial\epsilon}{\partial N}\right)_Y=\frac{1}{v^o}\int_{P_o}^{P_i}v(P)\mathrm{d}P. \tag{17}$$

The upper integration limit (P_i, see Eq. (15)), is matched so as to fulfill Eq. (17), which is equivalent to putting the pressure value P_i in the field equal to the local total pressure value $P_o+\Pi$

$$-\frac{N^o}{\epsilon_o}\left[\left(\frac{\partial f}{\partial Y}\right)\left(\frac{\partial Y}{\partial\epsilon}\right)\right]_{\zeta_L}\left(\frac{\partial\epsilon}{\partial N}\right)_Y=\frac{1}{v^o}\int_{P_o}^{P_o+\Pi}v(P)\mathrm{d}P, \tag{18}$$

The meaning of the above Eq. (18) written in this way is that the external pressure P_i applied without electric field would produce water compression comparable to that due to the total local pressure equal to the external pressure P_o plus the electrostriction pressure Π. Note that a similar position has also been adopted by other authors, e.g., a neutron scattering experiment with isotopic substitution on a 10 M NaOH solution was interpreted as to "indicate that ions in aqueous solutions induce a change in water structure equivalent to the application of high pressure" [27].

From Eq. (18) taking into account Eq. (6) one obtains the following form of *the equation of state* of H_2O

$$\frac{V}{\epsilon_o}\left(\frac{\partial}{\partial\epsilon}\int_0^Y\frac{\sigma}{\epsilon}\mathrm{d}y\right)\left(\frac{\partial\epsilon}{\partial N}\right)_{T,V,\sigma}=\int_{P_o}^{P_o+\Pi}\frac{\partial V}{\partial N}\mathrm{d}P. \tag{19}$$

Π in the upper limit of the rhs integral represents the only unknown quantity in Eq. (19). Eq. (19) represents the equation of state of H_2O in Π, σ and T variables, of which T is implicit. The dependence on temperature is present through the relation $\epsilon=\epsilon(T)$ as expressed in Eqs. (B.4), (B.6) and (12) and through the introduction into Eq. (18) of the isotherm $v=v(P)$ for the same temperature T for which ϵ is calculated. The dependence on the electric field strength E is present through f and Y (cf. Eqs. (2) and (6)). Since the actual dependence of the volume $V=V(P_o+\Pi)$ on the total local pressure ($P_o+\Pi$) is not available, the isotherms $V=V(P)$ of H_2O under pressure P applied in the absence of an electric field [28] are used instead. This approximation can be substantiated *a posteriori* as has been done with a positive result in Refs. [20,26].

3. Discontinuous and continuous phase transitions of H_2O in high electric field under pressure

To attain the goals of the current work, calculations have been performed for external pressures of $10^{-4} \le P_o \le 0.8$ GPa. It will be shown that under lower external pressures both the already described discontinuous phase transition of water in high electric field and a newly predicted continuous one are encountered, while under higher external pressures only the continuous one persists.

3.1. First-order phase transition and electric critical point of H_2O in the plane of surface charge density and pressure

In earlier papers [14,15] we have presented theoretical evidence for the electric-field-induced phase transition of water in a high electric field (10^9 V m^{-1}) at the atmospheric pressure ($P_o = 10^{-4}$ GPa) at temperatures in the range $273 < T < 303$ K. No discontinuity has been found above the electric critical temperature $T_c^E = 308 \pm 5$ K. Herein we ask the question what happens to these electric-field-induced phase transitions when the system under investigation is exposed to a high external pressure P_o. The calculations of this subsection have been performed for pressures in the range $10^{-4} < P_o < 0.06$ GPa with a step of 0.01 GPa at temperature $T = 293$ K, as well as for $P_o = 0.1$ and $P_o = 0.2$ GPa in the temperature range $273 < T < 373$ K changed every 10 K. Permittivity values $\epsilon = \epsilon(\sigma)$ of water as a function of surface charge density σ are found as described in Appendix B and are shown in Figs. 1, 2 and 3. In Ref. [15] (Fig. 2 therein) an isotherm Π vs. σ of water at 293 K at atmospheric pressure has been plotted with a straight horizontal segment testifying to the coexistence of two different phases. This line is also seen in the current Figs. 4 and 5 as the lowest isobar. Now, what happens to it under slightly higher pressures? Under pressures applied, the phase transition of water in a high electric field extends at 293 K to the pressure range 10^{-4}–0.05 GPa and has the discontinuous (first order) character (Fig. 4). The region of coexistence of two phases, B and A, of H_2O extends up to a critical point C (Fig. 5). It is termed "electric" critical point to discern it from the usual one related to the water-vapour system. The parameters defining the position of the electric critical point C are bound according to the set of inequalities shown in Eq. (20)

$$\begin{aligned} &0.276 \le \sigma_c \le 0.277 \text{ C m}^{-2}, \\ &0.05 \le P_c^E \le 0.06 \text{ GPa}, \\ &0.245 \le P_c^E + \Pi_c \le 0.26 \text{ GPa}, \end{aligned} \tag{20}$$

where the value of P_o at the criticality – the "electric" critical pressure (not to be confused with the ordinary critical pressure

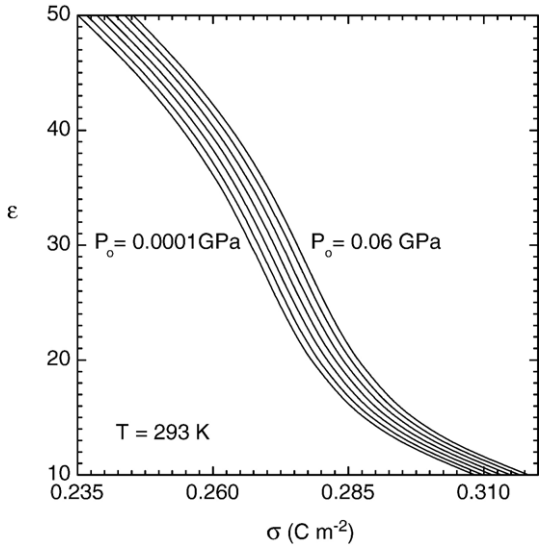

Fig. 1. Electric permittivity ϵ of water as a function of the surface charge density σ at 293 K at the pressures $P_o = 10^{-4}$, 0.01,0. 02,..., 0.06 GPa applied (from the lowest one upwards). The lowest line at 10^{-4} GPa has independently been confirmed by Monte Carlo calculations in Ref. [42] (see Fig. 7 therein).

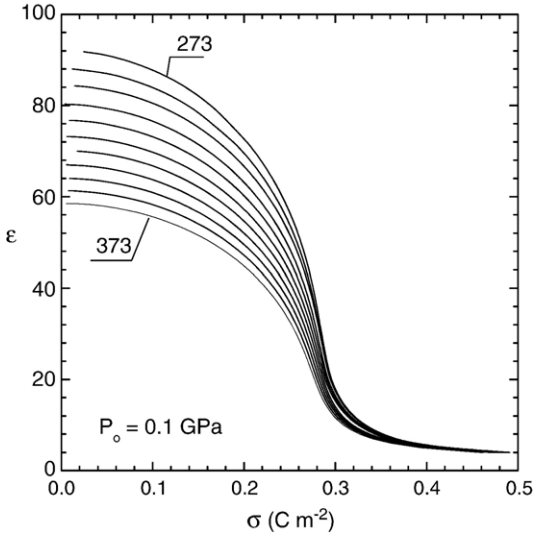

Fig. 2. Electric permittivity ϵ of water as a function of the surface charge density σ at the pressure $P_o = 0.1$ GPa applied in the temperature range $273 \le T \le 373$ K.

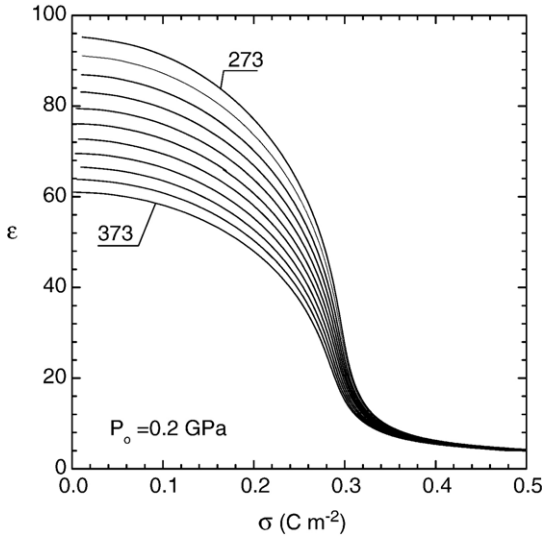

Fig. 3. Same as Fig. 2 at pressure $P_o = 0.2$ GPa applied.

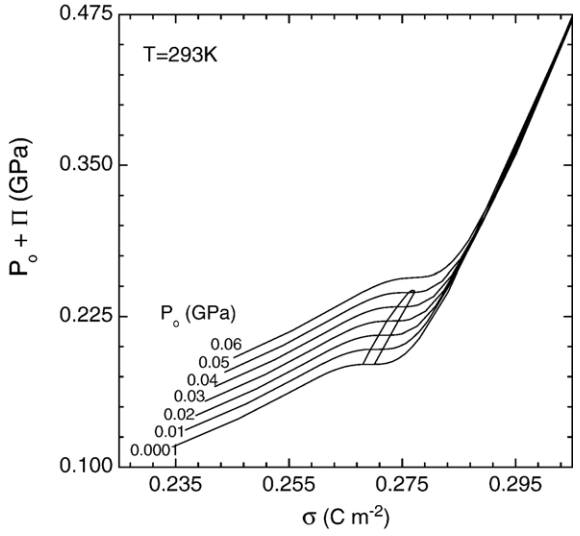

Fig. 4. Pressure $(P_o+\Pi)$ — the sum of the pressure P_o applied and the electrostriction pressure Π — acting on water in the electric field, plotted as a function of the surface charge density σ at 293 K. The seven lines correspond to $P_o=10^{-4}$, 0.01, 0.02..., 0.06 GPa. A contour is drawn around the region of coexistence of two phases B and A (not marked) of water in the electric field (see text).

of water in the P, V, T coordinates) – is denoted P_c^E. In Figs. 4 and 5, for $10^{-4}\le P_o\le 0.05$ GPa, there are apparent straight horizontal segments, characteristic of a region of phase coexistence. Along these segments, the pressure $(P_o+\Pi)$ acting on H_2O maintains a constant value of $(P_o+\Pi)_{t1}$, the transition pressure. This is equivalent to saying that the surface charge density σ (or the field E) as a function of the pressure $(P_o+\Pi)$ shows a discontinuity. Since the electric field E as a thermodynamic variable is the first derivative $\partial\Omega/(V\partial y)$ of the grand potential Ω as a function of polarization (cf. Eq. (5)), the discontinuity corresponds to the first order transition.

The isotherms under higher external pressures, exceeding P_c^E, namely $P_o=0.1$ and $P_o=0.2$ GPa and $273<T<373$ K are shown in Figs. 6 and 7. In the latter two plots, in contrast to the situation below P_c^E, no region of coexistence of phases B and A appears. In Figs. 6 and 7 the only remnants of this region are seen in the changes in slope of the isotherms with increasing surface charge density σ.

Let us characterize the phases B and A. To this aim, in Table 1 we have collected the data concerning six straight horizontal segments, characteristic of a region of phase coexistence, plotted in Fig. 5. The second and third columns in Table 1 show the values of σ at the low-field and high-field boundaries of the two-phase coexistence region. The fourth and fifth columns provide the values of ϵ_B and ϵ_A of the phases B and A, respectively, at the low-field and high-field boundaries of this region. The permittivity values plotted in Fig. 1 for σ within this region can be interpreted as weighted averages of ϵ_B and ϵ_A dependent on the quantity of either phase. The phases B and A differ in their dielectric properties, best characterized by their permittivity ϵ, since as, seen in Table 1, the difference in permittivity values between them under not-too-high pressures amounts to about 2 and vanishes only at the electric critical pressure P_c^E. At the same time, the mean cosine $\langle\cos\theta\rangle$ in the phases B and A is close to vanishing, and the difference in its values between these phases is even lower.

3.2. Second order phase transition of H_2O in high electric field

3.2.1. Discontinuity in the electrostriction pressure coefficient γ of water

Yet another aspect of isothermal relations between $(P_o+\Pi)$ and σ calculated on the basis of the equation of state Eq. (19) will now be discussed. Namely, two ranges with distinctly different slopes of the pressure $(P_o+\Pi)$ as a function of σ can be discerned. The total pressure $(P_o+\Pi)$ at the temperature $T=293$ K and under pressure applied in the range $10^{-4}\le P_o\le 0.8$ GPa (Fig. 8) and, on an extended scale, in the range $10^{-4}\le P_o\le 0.06$ GPa (Fig. 4), is plotted as a function of σ. From Figs. 8 and 4, the slope γ of $(P_o+\Pi)$ vs. σ defined as

$$\gamma=\left(\frac{\partial\Pi}{\partial\sigma}\right)_{P_o,T}. \tag{21}$$

can be derived. Eq. (21) defines the electrostriction pressure coefficient γ in an open system of H_2O in the electric field. P_o does not vary along any of the isotherms and does not affect the value of γ. On the left-hand sides of the two Figs. 4 and 8, at lower values of σ, the slope γ is low, while on the right-hand sides, at higher values of σ, the slope γ takes abruptly distinctly higher values. From Figs. 4 and 8, the values of σ_{t2} and $(P_o+\Pi)_{t2}$ can be read out for which the slope γ shows abrupt changes. At the pressure values $(P_o+\Pi)_{t2}$ shown, γ reveals discontinuities (jumps) for the σ_{t2} values as exemplified in Table 2. These jumps reveal the transition between the phase A with orientational disorder and the ordered phase OR. It is worth noting that the

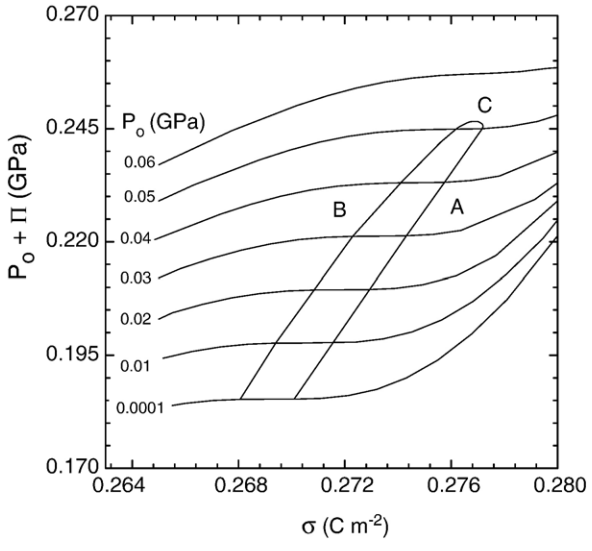

Fig. 5. Portion of Fig. 4 on an extended scale to make apparent the details of the region of coexistence of phases B and A of water. The highest point, marked C, of the contour surrounding the region of coexistence is the electric critical point (cf. Eq. (20)). The straight horizontal segments within the contour reveal the discontinuity in the variable σ corresponding to the states with coexisting phases B and A at $T=293$ K.

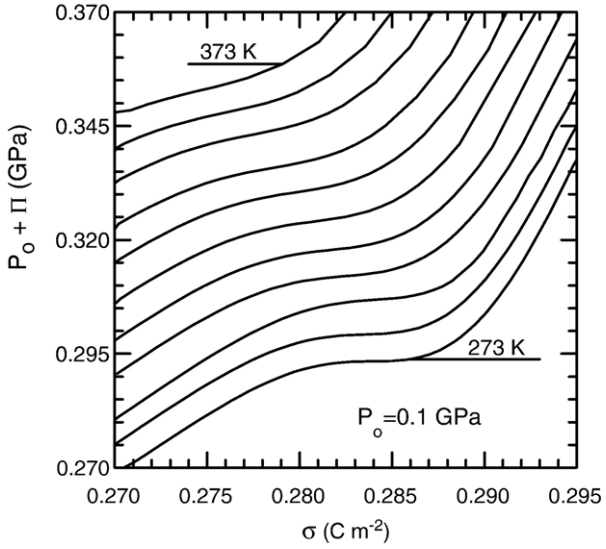

Fig. 6. Eleven isotherms of the sum of P_o=0.1 GPa and electrostriction pressure Π as a function of surface charge density σ are plotted for every 10 K for temperatures from 273 K up to 373 K.

jump of γ occurs at a value of permittivity ϵ_{t2}=25 independent of pressure. This can be well seen in Fig. 9, showing the electric permittivity ϵ as a function of the total pressure $(P_o+\Pi)$ for various external pressures P_o. The values of the transition pressures $(P_o+\Pi)_{t2}$ at the crossings with the isotherms (full lines) at 293 K for various P_o given in Table 2 are joined by the dashed line. It is clear that the dashed line is horizontal and its ordinate amounts to ϵ_{t2}=25.

The jump in the electrostriction pressure coefficient γ represents the discontinuity of the first derivative of pressure or, equivalently, of the second derivative of the thermodynamic potential. Thus, for the values of σ_{t2} and $(P_o+\Pi)_{t2}$ given in Table 2, the discontinuity of γ is related to the second order (continuous) transition.

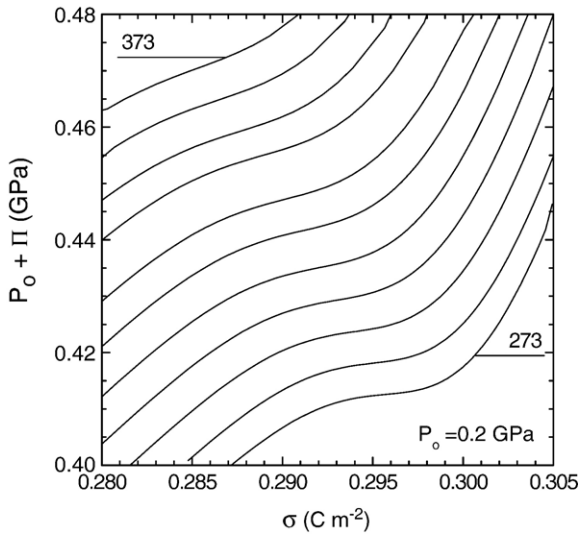

Fig. 7. Same as Fig. 6 at P_o=0.2 GPa.

Table 1
Data concerning the discontinuous phase transition under various pressures P_o applied (Fig. 5)

P_o	σ_B	σ_A	ϵ_B	ϵ_A	$(P_o+\Pi)_{t1}$
GPa	C m^{-2}	C m^{-2}			GPa
10^{-4}	0.268	0.270	29	27	1.85
0.01	0.269	0.2715	29	27	1.98
0.02	0.271	0.273	29	27	2.09
0.03	0.2723	0.2743	29	27	2.21
0.04	0.2743	0.2757	28	27	2.33
0.05	0.276	0.277	28	27	2.45

σ_B (σ_A) denote the surface charge density values at low-field (high-field) boundary, respectively, of the two-phase region. ϵ_B (ϵ_A) denote the permittivity values at the respective boundaries of the two-phase region. P_o is the pressure applied, $(P_o+\Pi)_{t1}$ is the total pressure at the transition and Π is the electrostriction pressure.

3.2.2. Order parameter

We have noted that the discontinuity of γ occurs at a specific value of the permittivity ϵ_{t2}. On the other hand, ϵ is related (Eq. (B.4) in Appendix B) to $\langle\cos\theta\rangle$, the mean value of the cosine of the angle between the field E and the dipole moment μ of a water molecule. Taking into account Eqs. (B.6) and (B.1), we have calculated $\langle\cos\theta\rangle$ in normal conditions and plotted it as a function of σ in Fig. 10. As follows, $\langle\cos\theta\rangle$ is close to zero below σ_{t2}=0.2721 C m^{-1} (cf. Table 2) corresponding to the discontinuity of γ, while for higher σ values $\langle\cos\theta\rangle$ takes finite values. At higher electric fields (or σ) the mean cosine $\langle\cos\theta\rangle$ tends to its saturation value of unity. In view of the above, $\langle\cos\theta\rangle$ can be considered as the *order parameter* of water in the field, related to the second order transition at σ_{t2}. Fig. 11 shows $\langle\cos\theta\rangle$ at two different temperatures (293 K and 333 K), while Fig. 12 shows $\langle\cos\theta\rangle$ as a function of σ under three different external pressures P_o (atmospheric, 0.3 GPa and 0.6 GPa). As seen in the examples in Fig. 11 the transition value σ_{t2} seems to

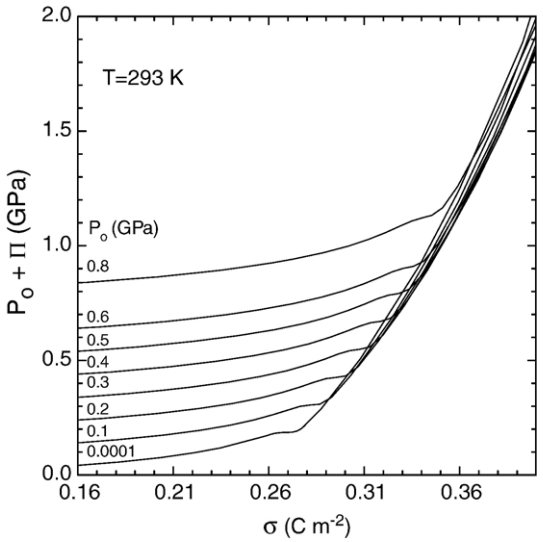

Fig. 8. Same as Fig. 4, but for higher values of $(P_o+\Pi)$. The numbers on the left-hand side of the plot are different values of the pressure P_o applied of the individual lines. The lowest line at 10^{-4} GPa has independently been confirmed by Monte Carlo calculations in Ref. [42] (see Fig. 9 therein).

Table 2
Values of the pressure P_o applied, surface charge density σ_{t2}, total pressure $(P_o+\Pi)_{t2}$ and electrostriction pressure Π_{t2} for which the electrostriction pressure coefficient γ is discontinuous at 293 K and the permittivity $\epsilon_{t2}=25$

P_o	σ_{t2}	$(P_o+\Pi)_{t2}$	Π_{t2}
GPa	C m^{-2}	GPa	GPa
10^{-4}	0.2721	0.1861	0.1860
0.01	0.2735	0.1986	0.1886
0.02	0.2750	0.2106	0.1906
0.03	0.2764	0.2225	0.1925
0.04	0.2778	0.2345	0.1945
0.05	0.2792	0.2466	0.1966
0.06	0.2806	0.2597	0.1997
0.1	0.2867	0.3080	0.2080
0.2	0.3003	0.4319	0.2319
0.3	0.3128	0.5580	0.2580
0.4	0.3240	0.6845	0.2845
0.5	0.3335	0.8100	0.3100
0.6	0.3412	0.9329	0.3329
0.8	0.3510	1.1653	0.3653

be independent of temperature, whereas in the example in Fig. 12 it seems to be higher under higher pressures P_o applied.

3.2.3. Water properties at either side of the transition

Let us summarize the properties of water forming an open system in the electric field at both sides of the second order phase transition. The phases B and A with $\langle\cos\theta\rangle \cong 0$, and hence having dipoles with disordered orientations, at a surface with surface charge densities $\sigma<\sigma_{t2}$ (Table 2), have the permittivity $\epsilon>25$. The relative mass densities d of phases B and A increase very slowly with increasing σ (Fig. 13) but for low σ distinctly depend on the pressure P_o applied. The discontinuous transition B→A is not accompanied by any significant increase in either $\langle\cos\theta\rangle$ or d. As mentioned above, the values of the permittivity ϵ differ by about 2 at the transition B→A. The transition A→OR occurs when $\langle\cos\theta\rangle$ and d start to increase markedly with σ at σ_{t2}; in the same conditions the electrostriction pressure coefficient γ as well as the derivative of the mass density $(\partial d/\partial\sigma)_{P_o,T}$ reveal jumps, and the electric permittivity attains the value $\epsilon_{t2}=25$. The mean cosine $\langle\cos\theta\rangle\neq 0$ for the surface charge densities $\sigma>\sigma_{t2}$ (cf. Table 2), increases with σ in the phase OR with $\epsilon<25$

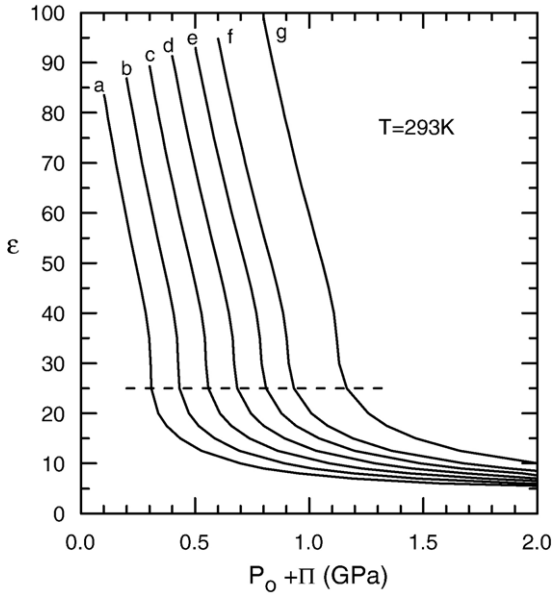

Fig. 9. Electric permittivity ϵ of water at various external pressures P_o as a function of the total pressure $(P_o+\Pi)$ at 293 K. Full lines marked with letters a, b, …, g are plotted at external pressures P_o: a — $P_o=0.1$ GPa, b — 0.2 GPa, c — 0.3 GPa, d — 0.4 GPa, e — 0.5 GPa, f — 0.6 GPa, g — 0.8 GPa, respectively. The horizontal dashed line corresponds to the value of $\epsilon_{t2}=25$ at the transition: phase A ⇔ phase OR.

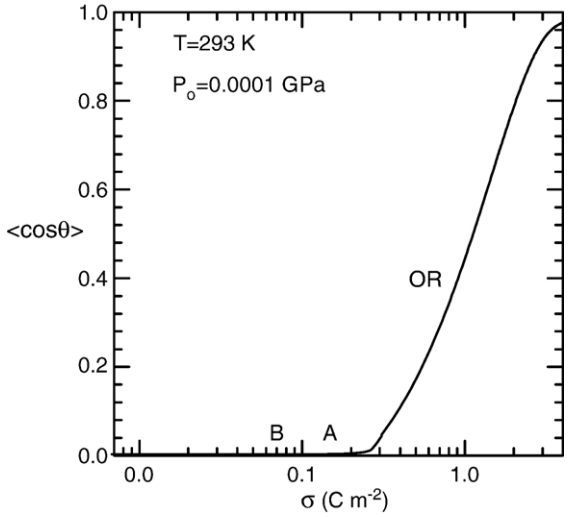

Fig. 10. The mean cosine $\langle\cos\theta\rangle$ of the angle θ between the direction of the electric field E and the electric dipole moment μ of the water molecule as a function of the surface charge density σ (log scale) at an adjacent surface at atmospheric pressure P_o at ambient temperature. Letters B, A and OR mark the corresponding phases along the line.

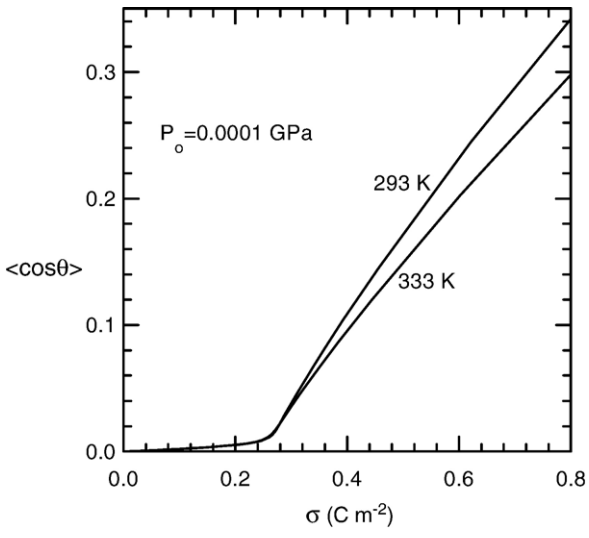

Fig. 11. The mean cosine $\langle\cos\theta\rangle$ of the angle θ between the direction of the electric field E and the electric dipole moment μ of the water molecule as a function of surface charge density σ at atmospheric pressure at two temperatures: $T=293$ K and $T=333$ K.

revealing orientational order and at the same time the mass density d is enhanced, eventually reaching values as high as 2 and higher (cf. Ref. [4,5,20]). Once the relative density d attains so high values for $\sigma > \sigma_{t2}$, it becomes only weakly dependent on external pressure P_o. From the point of view of the experiment, it is remarkable that there exist threshold values of the electric field $E_{t2} = \sigma_{t2}/(\epsilon\epsilon_o)$ with $\epsilon = 25$ (see Table 2), above which the process of making water more dense becomes noticeable. This threshold occurs at the second order transition discussed in this subsection. The necessity to overcome this threshold makes it conceivable why the dense water in the electric field has up to now been observed only in a few experiments [4–6,8,32]. Note that the dense water in the electric field in an open system in thermodynamic equilibrium should not be confused with the concept of high density water in the supercooled water in a metastable regime (see, for example, Ref. [33] and references therein). Under external pressures $P_o < 0.05$ GPa, below the electric critical point C (Fig. 5), the jump of γ occurs at the boundary of the phase A and the phase OR with orientational order. It follows from the data of the mean cosine (Fig. 10) that both phases A and B reveal almost no orientational order of dipoles of H_2O molecules in comparison with that of the phase OR. The values of $\langle \cos\theta \rangle$ of the phase A are slightly larger than those of the phase B, whenever the latter is discernible from A, while both remain marginally small.

4. Discussion

Experimental data on thermal phenomena in water [1,2] and its density and structure [3–8,25,32] at polar or charged surfaces are rather scarce. Since we attempted in the current work to present a theory that in the limit of atmospheric pressure gives account, to some extent, of these experiments, it seems natural

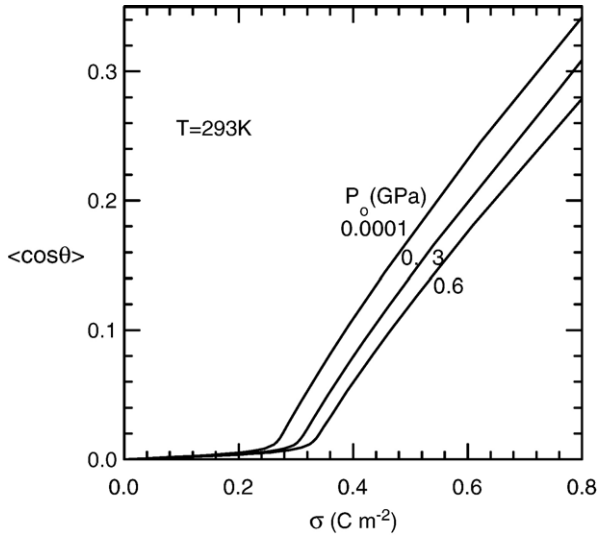

Fig. 12. The mean cosine $\langle \cos\theta \rangle$ of the angle θ between the direction of the electric field E and the electric dipole moment μ of the water molecule as a function of surface charge density σ at three different pressures P_o (10^{-4}, 0.3 and 0.6 GPa).

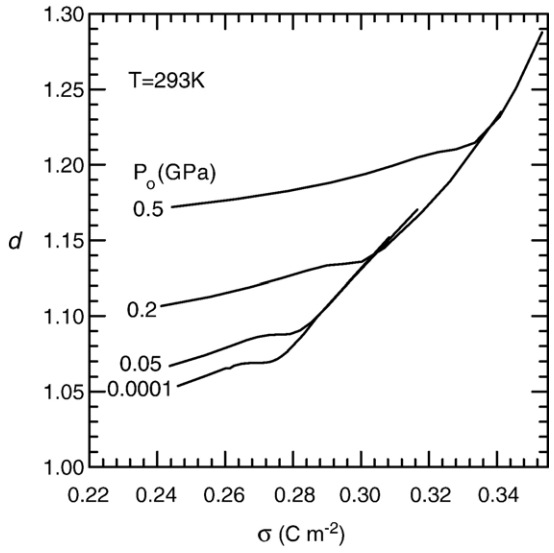

Fig. 13. Plot of the relative mass density d of water as a function of surface charge density σ under various external pressures $P_o = 10^{-4}$, 0.05, 0.2 and 0.5 GPa applied at ambient temperature.

to relate it with other theoretical approaches describing such or similar situations. We will mention three topics:

1. Theory of phase transitions in two-dimensional models of systems of dipoles and the related experiment.
2. Experiments testifying for or against the fluid nature of the phases considered in the current work.
3. Molecular dynamics studies of aqueous systems at a charged or polar wall.

Some theoretical approaches, as exemplified by Refs. [29–31], have undertaken the question of structural phase transitions of water at interfaces. These theories [29–31] reported on transitions in two-dimensional closed model systems composed of dipole moments in the electric field. They were relatively successful in describing the thermal phenomena at mercury electrodes observed by Benderskii et al. [1,2]. How do they compare with our current work? Since in the region of phase coexistence no change in the values of the total pressure occurs (Figs. 4 and 5), at the transition pressure there are no dipolar molecules entering the high field region with increasing field — the process of the pull of additional dipoles into the field is blocked. Water in the high electric field at an electrode forms an open system, but in this specific range of physical parameters it mimics to some extent a closed one. This may eventually help to understand, from our point of view, the results of Refs. [29–31].

Let us point out that on purely thermodynamic grounds one cannot decide upon the structure of phases, or whether a phase is solid or fluid. Nevertheless, we admit the possibility of liquid–liquid transitions. Such transitions are not unknown: there exist phase boundaries in the (P, T) plane for quantal (^{4}He, ^{3}He and H) and "classical" elemental liquids (C, P, Se, S) characterized by a change in the local coordination number across these boundaries [38]. The experiments have not resolved the question of the nature of the dense phase in the

high electric field (our OR phase) yet. Interpretation of measurements by Kasinski et al. [3] suggests the presence of a solid dense phase in the high electric field, while the viscosity–density product studies by Plausinaitis et al. [39] do not exclude the existence of a dense fluid in such conditions, however at thicknesses higher than the first few molecular layers at an electrode. The experiment by Choi et al. [7], in the light of their Errata, does not seem to resolve this question, too.

Some theoretical approaches apply several models of water to study its properties at polar or charged surfaces by the molecular dynamics (MD) simulation method. An account of the early work on water at interfaces, including MD simulations, can be found in Ref. [34]. MD simulations of water at charged electrodes have been performed by Yeh and Berkovitz as well as by Crozier et al. [35,36]. Yet these simulations appeared unable to reproduce quantitatively the experimental data on local mass density profile at a charged wall by Toney et al. [4,5], whereas our approach [37] (the same as the current one) was able to account for it with no use of adjustable parameters. Note that the latter paper deals with the density profile – the mass densities of consecutive water layers at a wall – profiting from the fact that within our approach one can calculate local quantities and not only those concerning a uniform medium. In the light of the new results presented herein one can offer a new interpretation of the previous results [4,5,20,37]. Namely, at ambient conditions, water layers in the high electric field at an electrode with densities distinctly exceeding unity (say, ≈ 1.2 or more) should be attributed to the oriented phase OR discussed herein. Moreover, as follows from our calculations, this enhanced density characteristic of the phase OR should persist under high pressures applied, but this requires experimental verification. Let us still remark that in the last decade, to our best knowledge, no serious criticism has been published of Toney et al.'s [4,5] results. Also, so far as we know, no MD simulation papers presenting a quantitative agreement with the mass density profile found experimentally at a charged electrode appeared recently.

In the last decade, the number of MD work on the problem of water at a wall has increased significantly (see, for example, references in Ref. [40]). So far as it is possible, a qualitative comparison would be instructive of our current results with those of the exemplary very recent paper by Giovambattista et al. [40], notable by taking into account both the effect of pressure and that of a polar surface on water, which also is the question dealt with herein. The two model solid plates in Ref. [40] are assumed to have fixed positions of ions, and hence a fixed polarity. Also, a fixed number N of molecules (closed system) is admitted. On the other hand, we discuss a single plate with varied polarity (or equivalent surface charge density), and confinement effects are avoided. Also, an open system with a varying number N of molecules within the reach of the field is considered herein. All that makes a direct comparison somewhat uncertain. One of the findings of the authors of Ref. [40] is that the density profile of water as a function of distance from one of the two parallel hydrophilic plates is "insensitive to [pressure] P over the range of conditions investigated", which means $T=300$ K and $P \leq 0.2$ GPa. On the other hand, we are led to a conclusion that for some surface charge density σ values, the local mass density d (or mass density profile) depends noticeably on the pressure P_o applied (Fig. 13). However, in Fig. 13 specific values of σ can be found for which the value of d is the same for different P_o. The examples are situated at the crossings of the isobars: for $\sigma=0.287$ C m^{-2} and two pressures $P_o=10^{-4}$ and 0.05 GPa as well as for $\sigma=0.304$ C m^{-2} and pressures $P_o=0.05$ and 0.2 GPa applied. Close to such points the pressure dependence of d is weak, which formally corresponds to the cited result (insensitivity to pressure) in Ref. [40], but it may well be accidental.

One of the reasons why a reconciliation of the MD results with the other ones is difficult can be the quantum nature of the H-bonds, as pointed out a decade ago by Brodsky in his essay on the predictive "value" of water computer simulations [41], which seems valid to some extent even today.

5. Summary

Let us summarize our results concerning the phase diagram of liquid water under the simultaneous action of high electric field and pressure. The picture that emerges herein is to some extent apparent in Figs. 4, 5 and 8. Going from the left hand side characterized by relatively moderate electric fields (or, which is more convenient at a charged surface, moderate surface charge densities σ) towards higher electric fields, at first normal water (termed, at atmospheric pressure, phase B in Ref. [15]) is encountered. We apply this nomenclature also for water under external pressure applied. Next, going to higher values of σ along any isobar at 293 K under pressures 10^{-4}–0.05 GPa applied, one faces the first-order phase transition. We have already considered a similar 1st order transition [14,15] for temperatures in the range $273<T<313$ K; it was positively related to a thermal effect found in literature [1,2]. Herein, it is found that the transition extends to higher pressures applied. This phenomenon is bounded from above by the electric critical pressure P_c^E ($0.05<P_c^E<0.06$ GPa) at 293 K. An experimental check could rely upon finding a related thermal effect, like that found in Ref. [1,2], but observed under pressure. On going further to the right (higher σ values) the contour seen in Figs. 4 and 5 is crossed (or circumvented, if above the critical point C, where the phases B and A merge) and the phase A is entered. When one continues towards higher σ (or electric field) values, one reaches an abrupt change in slope of the isobar, seen in Figs. 4 and 8. This abrupt change (cf. the data in Table 2) indicates the second order phase transition from phase A to phase OR characterized by high values of the coefficient γ, non-zero values of the order parameter $\langle\cos\theta\rangle$ (Fig. 10), and able to be easily compressed by the electric field and thus to attain higher and higher mass densities (Fig. 13).

We conclude with indicating that we have attained two goals. Firstly, we have predicted two phase transitions of water in a high electric field: a discontinuous one and, at higher electric fields, a continuous one. The latter occurs at a threshold value of the electric field and leads to a dense phase of thin layers of water (below 1 nm) with oriented dipoles. Secondly, we predict what will happen to these phase transitions of H_2O in high electric field under externally applied pressure. In particular, the

first order phase transition will vanish at a certain critical value of external pressure P_c^E. The second order phase transition persists at all pressures considered if the permittivity of H_2O reaches the value $\epsilon=25$.

The results give account of different thermal and scattering experiments on thin layers of water in very high electric fields, as encountered in many physical and biological systems. Analogous experiments performed under pressure would be welcome.

Appendix A

In this Appendix we provide some details of the calculation of the lhs of Eq. (18), which is the same as the rhs of Eq. (10). The first factor in the form of a derivative on the rhs of Eq. (10) is

$$\frac{\partial f}{\partial Y}=\frac{\sigma}{\epsilon}. \tag{A.1}$$

With the value of σ taken from Eq. (3) one obtains:

$$\frac{\partial f}{\partial Y}=\frac{q}{4\pi\epsilon x^2}=\frac{qX}{4\pi\epsilon}, \tag{A.2}$$

where $X=x^{-2}$. The second factor can be written as

$$\frac{\partial Y}{\partial \epsilon}=\frac{q}{4\pi}\left[\left(\frac{\partial X}{\partial \epsilon}\right)\left(1-\frac{1}{\epsilon}\right)+\frac{X}{\epsilon^2}\right]. \tag{A.3}$$

The derivatives: the third factor $(\partial\epsilon/\partial N)$ in Eq. (10) and $(\partial X/\partial\epsilon)$ in Eq. (A.3) will be calculated in a way similar to that explained in Ref. [15]. From an expression obtained in Ref. [17] for permittivity ϵ as a function of the field strength E and temperature T (cf. Eq. (B.4) below) we obtain the derivatives occurring in Eqs. (10) and (A.3):

$$N^o\left(\frac{\partial\epsilon}{\partial N}\right)_y=\frac{\frac{B}{VX(I-1)}\left(I\coth\frac{I\Xi}{I-1}-\coth\frac{\Xi}{I-1}\right)}{\frac{n^2}{\epsilon^2}-\frac{BA}{VT(I-1)^2(\epsilon+n^2/2)^2}\left[I^2\left(\sinh\frac{I\Xi}{I-1}\right)^{-2}-\left(\sinh\frac{\Xi}{I-1}\right)^{-2}\right]}. \tag{A.4}$$

and

$$\frac{\partial X}{\partial\epsilon}=X^2\left\{\frac{V(I-1)n^2}{B\epsilon^2}-\frac{A}{T(I-1)(\epsilon+n^2/2)^2}\left[I^2\left(\sinh\frac{I\Xi}{I-1}\right)^{-2}-\left(\sinh\frac{\Xi}{I-1}\right)^{-2}\right]\right\}\times\left\{\left(\coth\frac{\Xi}{I-1}-I\coth\frac{I\Xi}{I-1}\right)+\frac{AX}{T(I-1)(\epsilon+n^2/2)}\times\left[\left(\sinh\frac{\Xi}{I-1}\right)^{-2}-I^2\left(\sinh\frac{I\Xi}{I-1}\right)^{-2}\right]\right\}^{-1} \tag{A.5}$$

The quantities A (cf. Eq. (13)), B (cf. Eq. (B.5)) and the refraction index n are temperature dependent and found with the help of the data collected in [15], Table 2 therein.

Appendix B

In this Appendix it will be shown how to calculate the values of the mean cosine $\langle\cos\theta\rangle$ within our temperature interpolation scheme (cf. Ref. [17]). For small values of the argument Ξ the function $B_I(\Xi)$ (Eq. (11)) can be expanded into the power series:

$$B_I(\Xi)=\frac{I+1}{3(I-1)}\Xi-\frac{I^4-1}{45(I-1)^4}\Xi^3+\cdots\equiv b(I)\Xi-c(I)\Xi^3+\cdots \tag{B.1}$$

The coefficient $b(I)$ and the mean number of orientations I of the dipole moment are interrelated as (cf. Eq. (B.1))

$$b(I)=\frac{I+1}{3(I-1)}, \tag{B.2}$$

or inversely

$$I=\frac{3b+1}{3b+1}. \tag{B.3}$$

The relation between the permittivity ϵ and the electric field strength is, according to the Onsager field model [43], expressed as (cf. Ref. [15]):

$$\frac{\epsilon-n^2}{\epsilon}=\frac{B}{VX}\langle\cos\theta\rangle, \tag{B.4}$$

where

$$B=\frac{4\pi N\mu(n^2+2)}{3q}\,\mathrm{m\ kmol^{-1}} \tag{B.5}$$

and

$$\langle\cos\theta\rangle=B_I(\Xi). \tag{B.6}$$

In order to find the values of the permittivity ϵ in the high electric field E we look for $\langle\cos\theta\rangle=B_I(\Xi)$. To this aim, first the numerical value of $b(I)$ (Eqs. (B.1), (B.2), (B.3)) should be found in the linearized version of the Onsager approximation (cf. Ref. [17], Eq. (19) therein):

$$\frac{3(\epsilon-n^2)(2\epsilon+n^2)}{\epsilon(n^2+2)^2}=b(I)\frac{\mu^2N^o}{\epsilon_o vkT} \tag{B.7}$$

provided that the (field-independent) dielectric constant ϵ at a given temperature T and pressure P_o is known from experiment. In this way, the values of $b(I)$ are found at a given T (Table 1 in Ref. [17] and Table 1 in Ref. [18]). Subsequently, following Eq. (B.3) the values of $I=I(T)$ are found (cf. Table 1 in Ref. [17] and Table 1 in Ref. [18]). With the known values of $I(T)$, one finds $B_I(\Xi)$ with the help of Eq. (B.1).

References

[1] V.A. Benderskii, A.M. Brodsky, G.I. Velichko, L.I. Daikhin, N.S. Lidorenko, G.F. Muchnik, Dokl. Akad. Nauk SSSR 286 (3) (1986) 648.
[2] V.A. Benderskii, A.M. Brodskii, L.I. Daikhin, G.I. Velichko, in: B.E. Conway, J.O.'M. Bockris, R.E. White (Eds.), Modern Aspects of Electrochemistry, vol. 26, Kluwer/Plenum Publ. Corp, New York, 1994, p. 1, Chapter 1.
[3] J.J. Kasinski, L.A. Gomez-Jahn, K.J. Faran, S.M. Gracewski, R.J. Dwayne Miller, J. Chem. Phys. 90 (1989) 1253.

[4] M.F. Toney, J.N. Howard, J. Richer, G.L. Borges, J.G. Gordon, O.R. Melroy, D.G. Wiesler, D. Yee, L.B. Sorensen, Nature 368 (1994) 444.
[5] M.F. Toney, J.N. Howard, J. Richer, G.L. Borges, J.G. Gordon, O.R. Melroy, D.G. Wiesler, D. Yee, L.B. Sorensen, Surf. Sci. 335 (1995) 326.
[6] Y.S. Chu, T.E. Lister, W.G. Cullen, H. You, Z. Nagy, Phys. Rev. Lett. 86 (2001) 3364.
[7] E.-M. Choi, Y.-H. Yoon, S. Lee, H. Kang, Phys. Rev. Lett. 95 (2005) 085701; Errata ibid. 96 (2006) 039905.
[8] D.I. Svergun, S. Richard, M.H.J. Koch, Z. Sayers, S. Kuprin, G. Zaccai, Proc. Natl. Acad. Sci. U. S. A. 95 (1998) 2267.
[9] F. Merzel, J.C. Smith, Proc. Natl. Acad. Sci. U. S. A. 99 (2002) 5378.
[10] J.C. Smith, F. Merzel, Ch.S. Verma, S. Fischer, J. Mol. Liq. 101 (2002) 27.
[11] I. Danielewicz-Ferchmin, E. Banachowicz, A.R. Ferchmin, Biophys. Chem. 106 (2003) 147.
[12] I. Danielewicz-Ferchmin, E. Banachowicz, A.R. Ferchmin, ChemPhysChem 7 (2006) 2126.
[13] A. Amararene, M. Gindre, J.-Y. Le Huérou, W. Urbach, D. Valdez, M. Waks, Phys. Rev., E Stat. Phys. Plasmas Fluids Relat. Interdiscip. Topics 61 (2000) 682.
[14] I. Danielewicz-Ferchmin, A.R. Ferchmin, Chem. Phys. Lett. 398 (2004) 186.
[15] I. Danielewicz-Ferchmin, A.R. Ferchmin, ChemPhysChem 6 (2005) 1499.
[16] H.S. Frank, J. Chem. Phys. 23 (1955) 2023.
[17] I. Danielewicz-Ferchmin, A.R. Ferchmin, Phys. Chem. Chem. Phys. 6 (2004) 1332.
[18] E. Banachowicz, I. Danielewicz-Ferchmin, Phys. Chem. Liq. 44 (2006) 95.
[19] G.W. Toop, Metall. Mater. Trans., B, Proc. Metall. Mater. Proc. Sci. 26 (1995) 577.
[20] I. Danielewicz-Ferchmin, A.R. Ferchmin, J. Phys. Chem. 100 (1996) 17281.
[21] I. Danielewicz-Ferchmin, A.R. Ferchmin, Phys. Chem. Chem. Phys. 5 (2003) 165.
[22] I. Danielewicz-Ferchmin, A.R. Ferchmin, Phys. Chem. Liq. 42 (2004) 1.
[23] C. Kittel, Introduction to Solid State Physics, Wiley, New York, 1966 Chapter 14.
[24] J.S. Smart, Effective Field Theories of Magnetism, W.B. Saunders Co, Philadelphia, 1966 Chapter 1.
[25] Ph. Wernet, D. Nordlund, U. Bergmann, M. Cavalleri, M. Odelius, H. Ogasawara, L.Å. Näslund, T.K. Hirsch, L. Ojamäe, P. Glatzel, L.G.M. Pattersson, A. Nilsson, Science 304 (2004) 995.
[26] I. Danielewicz-Ferchmin, A.R. Ferchmin, Physica B 245 (1998) 34.
[27] F. Bruni, M.A. Ricci, A.K. Soper, J. Chem. Phys. 114 (2001) 8056.
[28] W. Wagner, A. Pruß, J. Phys. Chem. Ref. Data 31 (2002) 387.
[29] A.M. Brodskii, L.N. Daikhin, Elektrokhimiya 25 (4) (1989) 435 (English translation: Sov. Electrochem. 25 (1989) 379).
[30] S. Harinipriya, M.V. Sangaranarayanan, J. Colloid Interface Sci. 250 (2002) 201.
[31] S. Harinipriya, M.V. Sangaranarayanan, Indian J. Chem., Sect. A 42 (2003) 965.
[32] A. Harata, T.E. Lister, T. Sawada, Physica B 219–220 (1996) 629.
[33] A.K. Soper, M.A. Ricci, Phys. Rev. Lett. 84 (2000) 2881.
[34] J. Israelachvili, Intermolecular and Surface Forces, Academic Press, London, 1991.
[35] In-Chul Yeh, M.L. Berkowitz, J. Chem. Phys. 112 (2000) 10491.
[36] P.S. Crozier, R.L. Rowley, D. Henderson, J. Chem. Phys. 113 (2000) 9202.
[37] I. Danielewicz-Ferchmin, A.R. Ferchmin, A. Szlaferek, Chem. Phys. Lett. 288 (1998) 197.
[38] G.G.N. Angilella, F.E. Leys, N.H. March, R. Pucei, Phys. Chem. Liq. 41 (2003) 211.
[39] D. Plausinaitis, M. Waskaas, R. Raudonis, V. Daujotis, Electrochim. Acta 51 (2006) 6152.
[40] M. Giovambattista, P.J. Rossky, P.G. Debenedetti, Phys. Rev., E Stat. Phys. Plasmas Fluids Relat. Interdiscip. Topics 73 (2006) 041604.
[41] A. Brodsky, Chem. Phys. Lett. 261 (1996) 563.
[42] R.P. Joshi, J. Qian, K.H. Schoenbach, E. Schamiloglu, J. Appl. Phys. 96 (2004) 3617.
[43] C.J.F. Böttcher, O.C. Van Belle, P. Bordevijk, A. Rip, 2nd edn., Theory of Electric Polarization, vol.1, Elsevier, Amsterdam, 1973.